Formation of molecular hydrogen on analogues of interstellar dust grains: experiments and modeling

Gianfranco Vidali[1], Joe Roser[1], Giulio Manicó[2], Valerio Pirronello[2], Hagai B. Perets[3], and Ofer Biham[3]

[1] Syracuse University, 201 Physics Bldg., Syracuse, NY 13244-1130, USA
[2] Dipartimento di Metodologie Fisiche e Chimiche per l'Ingegneria, Universita' di Catania, 95125 Catania, Sicily, Italy
[3] Racah Institute of Physics, The Hebrew University, Jerusalem 91904, Israel

E-mail: `gvidali@syr.edu`

Abstract. Molecular hydrogen has an important role in the early stages of star formation as well as in the production of many other molecules that have been detected in the interstellar medium. In this review we show that it is now possible to study the formation of molecular hydrogen in simulated astrophysical environments. Since the formation of molecular hydrogen is believed to take place on dust grains, we show that surface science techniques such as thermal desorption and time-of-flight can be used to measure the recombination efficiency, the kinetics of reaction and the dynamics of desorption. The analysis of the experimental results using rate equations gives useful insight on the mechanisms of reaction and yields values of parameters that are used in theoretical models of interstellar cloud chemistry.

1. Introduction

The formation of molecular hydrogen in interstellar space is an important problem in astrophysics and astrochemistry. Molecular hydrogen is not only the most abundant molecules in the Universe, but it contributes to the initial gravitational collapse of a cloud by re-radiating in the infrared energy generated by the collapse and intervenes, either in its charged or neutral form, in virtually all reaction schemes leading to the formation of more complex molecules in the interstellar medium (ISM). The reasons why there has always been much interest in its formation is that molecular hydrogen needs to be continuously generated in space, since ultraviolet photons, cosmic rays, shocks and chemical reactions are the main agents contributing to its destruction, and that its formation in the gas phase is very inefficient. Although there are various routes to make molecular hydrogen, formation rates of reactions in the gas phase cannot produce it in enough quantities to explain its presence given the destruction rates of the processes mentioned above [1]. In the Sec. 2 we present a brief survey of the main developments in the studies of H_2 formation on interstellar dust grains over the past forty years or so. The early theories are reviewed in light of the constraints imposed by observations. The main results of laboratory experiments over the past decade and their implications are described. In Sec. 3 we review the reaction mechanisms on surfaces that are relevant to molecular hydrogen formation. The experiments performed in our laboratory are introduced in Sec. 4 and the results are presented in Sec. 5. These results are analyzed in Sec. 6. The implications and open problems are discussed in Sec. 7, followed by a summary in Sec. 8.

2. Formation of H$_2$ on interstellar dust grains

2.1. Review of early theories

Gould and Salpeter [2] showed that H$_2$ formation in the gas phase is not feasible and proposed that interstellar dust grains can act as catalysts in the formation of molecular hydrogen. In subsequent work, Hollenbach et al. showed that dust grains can successfully catalyze molecular hydrogen production at a rate which is compatible with its observed abundance [3, 4, 5]. The rate coefficient of molecular hydrogen formation R (cm^3 sec^{-1}) is related to the total number density of hydrogen atoms (both in atomic and molecular forms) $n = n_H + 2n_{H_2}$ and the photodissociation rate $\beta = 5 \times 10^{-10}$ (sec^{-1}) by: $Rn_H n = 0.11\beta n_{H_2}$ [6]. Jura calculated, based on an analysis of Copernicus observations in the local diffuse cloud medium, that the formation rate coefficient on grains is $10^{-17} < R < 3 \times 10^{-17}$ (cm^3 sec^{-1}) [7]. Since then, R has been measured in several different ISM environments. Remarkably, these analyses give a value of R very similar to the one estimated by Jura for local diffuse clouds. Recently, Gry et al. [8] have looked at the formation rate of H$_2$ in the diffuse ISM, using FUSE data, while Habart et al. [9] examined this rate in photodissociation regions, using SWS-ISO data. The reader is referred to these papers for a discussion of the mechanisms of formation of H$_2$ in these conditions.

To carry out the calculations, Hollenbach, Werner and Salpeter [3, 4, 5] made a number of assumptions, of which a couple turned out to be problematic: first, the calculation was done on grains coated with crystalline ice, since this was the understanding at that time, although later it was shown that most of ice in space is in the amorphous form and that the grains are bare in the diffuse cloud medium. Second, it was assumed that within the grain, hydrogen atoms moved from site to site by tunneling. Specifically, in each small crystal of ice, diffusion in the spatially periodic potential was by tunneling and very fast; Nonetheless, to prevent evaporation of atoms before they met each other, it was necessary to set the condition that the surface has enhanced binding sites beyond the weak ones. In any case, to make hydrogen formation likely over a range of temperature in the diffuse ISM, the H atoms cannot experience strong chemisorption forces, or otherwise there would be little migration of atoms out of the chemisorption sites. Under these assumptions, they arrived at the following expression for the recombination rate R_{H_2} (cm^{-3} sec^{-1}), namely the number of molecules formed per unit time and unit volume:

$$R_{H_2} = \frac{1}{2} n_H v_H \sigma \xi \eta n_g. \tag{1}$$

In this formula, n_H is the number density of hydrogen atoms, v_H is their speed, σ is the cross section of the grain, ξ is the sticking coefficient, η is the probability of bond formation once two atoms encounter each other and n_g is the number density of dust grains in the ISM. Assuming that the average sticking coefficient is $\xi = 0.3$, a result of their calculation of the interaction of a hydrogen atom with an ice surface, they obtained that they could recover the observed rate coefficient R of H$_2$ production if the probability of recombination of hydrogen atoms when on the surface was $\eta = 1$.

A dissenting voice was that of Smoluchowski [10, 11], who considered the problem of hydrogen atoms diffusing on an amorphous ice surface. Since tunneling is very sensitive, on an atomic scale, to the details of the environment through which a hydrogen atom diffuses, it is not surprising that in an amorphous medium the mobility is greatly reduced. Unfortunately, his calculations gave the result that the mobility of hydrogen atoms on an ice surface would be much too small to yield recombination events with the rate necessary to match observations.

An example of an alternative formation route for H$_2$ is the chemistry induced by charged particle bombardment of interstellar ices. Brown et al. conducted experiments where they sent MeV ions on water ice and measured the number of H$_2$O, H$_2$ and O$_2$ molecules, that were sputtered, or ejected in the gas-phase, per each impinging ion [12]. Using these experimental results, Avera and Pirronello evaluated theoretically the production rate of molecular hydrogen

per unit volume and time in dense interstellar clouds due to the bombardment of the icy mantles on grains by cosmic rays [13, 14]. The result they obtained was orders of magnitude higher than Smoluchowski's evaluation but much smaller than that of Hollenbach et al. [5].

Experiments on the formation of molecular hydrogen on surfaces were done since the work of Hollenbach and Salpeter, but these studies were carried out under conditions far enough from ISM conditions that they were of little use in elucidating the actual processes on dust grains. These studies are reviewed in Ref. [15].

2.2. Constraints on H$_2$ formation on dust grains

Consider the formation of molecular hydrogen in typical conditions found in diffuse or dense clouds. The gas-phase hydrogen atoms have kinetic energies below a few hundred K and grain temperature is low (< 20 K). Therefore, strongly bound (chemisorbed) atoms will be virtually immobile. Diffusion energy barriers, $E_{\mathrm{H}}^{\mathrm{diff}}$, are rather sensitive to the morphology of the surface. Roughly speaking, for weak adsorption sites $E_{\mathrm{H}}^{\mathrm{diff}} \sim E_{\mathrm{H}}^{\mathrm{des}}/5$, where $E_{\mathrm{H}}^{\mathrm{des}}$, is the binding energy of the atom. Strong adsorption sites have proportionally smaller diffusion energy barriers, namely $E_{\mathrm{H}}^{\mathrm{diff}} \sim E_{\mathrm{H}}^{\mathrm{des}}/20$. A typical grain of 0.1 μm radius, has an area $A \sim 10^{-9}$ cm^2, assuming that it is spherical (and considerably larger area for a rough surface). The number of adsorption sites on the grain is roughly $10^{15}A$ sites. There are a few timescales to consider: the time between arrivals, the residence time on the surface, and time between the arrivals of UV photons that can produce fluctuations in the temperature of the grain. The size of the grain, the porosity and the distribution of binding sites in energy are also important parameters. We now examine how these timescales are inter-related and what conditions we need to impose on the other parameters in order to have a reaction between two hydrogen atoms.

The arrival rate of H atoms on a grain is given by $n_{\mathrm{H}}v_{\mathrm{H}}\sigma$. A fraction ξ of the impinging atoms stick to the surface. For $n_{\mathrm{H}} = 100$ (atoms/cm^3) and $v_{\mathrm{H}} \sim 10^5$ (cm/sec), assuming gas temperature of about 100 K, one obtains that the collision rate of H atoms with a typical grain is ~ 1 particle per 300 seconds. The residence time is $t_{\mathrm{H}} = \nu^{-1}\exp(E_{\mathrm{H}}^{\mathrm{des}}/k_B T)$, where ν is the vibrational frequency (typically $\sim 10^{12}$ - 10^{13} sec^{-1}). E_H^{des} is the binding energy of the atom to an adsorption site on the surface, namely the activation energy barrier for desorption of the atom. Therefore, for $E_{\mathrm{H}}^{\mathrm{des}}/k_B \sim 500$ K, and surface temperature of $T \sim 10$ K, the residence time is $10^8 - 10^9$ (sec), but at higher temperatures around $T \sim 15$ K, t_{H} is reduced to the range of 30 to 300 (sec), which is comparable with the time between arrivals. The temperature of the grain is influenced by the ultraviolet (UV) photon flux. The time-scale for absorption of a photon is $t_{\mathrm{photon}} = (\sigma Q \Phi)^{-1}$ [16], where σ is the geometric cross section of the grain, Q is the absorption efficiency and Φ is the UV flux. In diffuse clouds, the average UV flux is 2.6×10^{-3} (erg cm^{-2} sec^{-1}) [17]. For large grains, the interval between absorption of photons is short (tens of seconds) and the grain will keep a stable temperature in the 15-20 K range. For smaller grains, the temperature fluctuations are in the range of 10 to 20 K for grain diameters $a \sim 0.01\mu$m, where $t_{\mathrm{photon}} \sim 750$ (sec), and in the range of 15 to 20 K for $a \sim 0.02\mu$m, where $t_{\mathrm{photon}} \sim 100$ (sec) [18]. In these cases and for even smaller grains, the arrival rate of particles is crucial since we need $\xi dN/dt > 1/t_{\mathrm{photon}}$ in order to maintain high efficiency of H$_2$ formation. It is clear that in this model the presence of H atoms on the surface is extraordinarily sensitive to the temperature of the grain, which in turn is related to its size, and that there is a rather narrow window when reactions can occur, as Hollenbach and Salpeter already pointed out [4].

The sensitivity to the conditions on the grains may be reduced by the fact that the surface of the grain may be porous enough that even if there is spontaneous desorption of H from a site there is a good chance that the H atom will strike another side of the grain and remain stuck to it. Also, there may be some density of sites with sufficient binding energy to confine H atoms for a long time. The distribution of sites might influence the formation of H$_2$ quite a bit. Furthermore, the broad grain-size distribution, namely by the fact that there are many more

small grains enhances the total surface area. The resulting increase in the collision rate between H atoms and dust grains may partly compensate for the low efficiency of H_2 formation.

2.3. Recent experiments and their implications

In the late 1990's, about thirty years after the work of Salpeter and collaborators, our group embarked on a program to measure how efficient the process of formation of molecular hydrogen on dust grains is, and whether, by recreating some of these processes in the laboratory, it is possible to learn about both the physical processes at play and the suitability of proposed dust grain analogues as replacements for the yet poorly known actual star dust material.

The first dust grain analogue that was used to test whether molecular hydrogen could be produced via processes described by the theory of Salpeter and collaborators was a polished polycrystalline olivine stone, a silicate. Silicates in space are mostly olivines, with a composition towards a magnesium-rich mineral, $(Mg_xFe_{1-x})_2SiO_4$ and x ranging from 1 for fayalite to 0 for fosterite [19]. The reason to choose olivine as a sample to study is that silicates are thought to be abundant in diffuse clouds, where the high destruction rate of molecular hydrogen makes it crucial that there exists an effective mechanism of formation. The results of our experiments, obtained with techniques and methods to be described below, were surprising [20, 21]. From the analysis of our data three main points stood out. First, the formation efficiency obtained from the data was a steep decaying function of the temperature of the sample at which the adsorption of hydrogen atoms took place. Second, for sufficiently high surface temperatures, the efficiency of recombination, defined here as the probability that two atoms hitting the surface would recombine, was lower than predicted by Hollenbach and Salpeter. Third, it was found that, for short exposure to atomic hydrogen so as to guarantee a sparsely populated fraction of H atoms on the surface of the dust grain analogue, the formation of molecular hydrogen obeyed second order kinetics and that the process of diffusion was assisted by thermal activation. The consequence of this finding was that for a range of high temperatures and low flux, the molecular hydrogen reaction rate must depend quadratically rather than linearly on the flux. Under such conditions the production rate is expressed by

$$R_{H_2} = n_g(n_H v_H \sigma \xi t_H)^2 \alpha/S, \tag{2}$$

where t_H is the residence time of an atom on the surface and α is the hopping rate of H atoms between adsorption sites and S is the number of adsorption sites on a grain. Here the expression in parenthesis is the coverage (average number of atoms adsorbed on the surface). Biham et al. found that whether the molecular hydrogen formation rate follows Hollenbach and Salpeter expression or ours depends on whether one is the situation of fast mobility (and/or high coverage) rather than slow mobility (and/or low coverage) of H atoms, respectively [22].

The next step was to measure the efficiency on an amorphous carbon sample [23], since amorphous carbon is one of the principal components of interstellar dust together with silicates [24]. The efficiency turned out to be higher than in the case of the polycrystalline sample and the TPD traces were broader in temperature, suggesting a range of activation energy barriers for the process of formation and ejection from the sample. Considering that the processes examined here are processes in which the atom/molecule - surface forces are weak and not very much dependent on the details of the chemical composition and arrangement of atoms of the solid, it is reasonable to expect that the differences in the recombination coefficients found in the two types of samples have to be related in a significant part to the different morphology. Finally, our group studied the efficiency and kinetics of molecular hydrogen formation [25, 26] on and the energetics [27] of molecular hydrogen ejection from the surface of water ice. Ice-coated grains are present in dense regions where most hydrogen is already in molecular form. Therefore, the study of the formation of molecular hydrogen on icy syrfaces does not have the same urgent interest that the formation on refractory materials that are exposed in diffuse clouds. However,

the study of processes of formation of molecular hydrogen on ice allows the easy manipulation of the surface, thus offering clues on the processes of hydrogen formation that in some cases might be extrapolated to other types of dust grains.

In an effort to study how the energy released in the molecular hydrogen reaction is distributed between the solid and within the nascent molecule, our group [27] and, independently, another group [28] measured the time of flight of molecules that were just formed on the surface and were being ejected from it. The next step, which is under way in our laboratory and elsewhere [29], is to study the distribution of the energy of the molecule within the roto-vibrational degrees of freedom. There are efforts under way to measure the excitation of the molecule in actual ISM environments; preliminary studies have not been successful, however, in singling out excitation of the molecules that can be ascribed to molecule formation events and not to pumping mechanisms due to shocks and photon absorption [30, 31].

3. Mechanisms of reactions at surfaces

Knowledge of the reaction steps is important in order to extract values of physical parameters that can be used then in modeling the chemistry of a cloud. The standard reaction scheme by which an impinging atom reacts with an atom adsorbed on a solid surface is the Langmuir-Hinshelwood (LH) mechanism [32]. In this reaction, the atom coming from the gas-phase becomes equilibrated with the surface, diffuses and, if it finds another atom, might react with it. Broadly speaking, we can identify the following steps in the reaction: sticking, diffusion, and reaction. In the sticking, the atom manages to loose its kinetic energy and becomes thermally accommodated on the surface. If there is a large mismatch between the mass of the incoming atom and the atom(s) of the surface, the transfer of energy is inefficient and the atom might bounce a few times on the surface before it becomes trapped. The energy of binding of the incoming atom with the surface depends greatly on the type of atoms and surface and on the way the interaction proceeds. For example, an atom approaching a surface will first experience an attractive long-range potential of the form $-C_3/z^3$, where z is the coordinate perpendicular to the surface and C_3 is a coefficient which depends on the atomic polarizability and dielectric response of the solid [33]. As the atom moves along the reaction coordinate it might get trapped in a shallow (typically < 500 K) potential well (physisorption) or it might get closer to the surface and, taking advantage of energetically favorable overlap of electronic orbitals, it might form a stronger bond ($>> 500$ K) with atoms on the surface (chemisorption). Whether the incoming particle will end up in a weak or strong adsorption site might depend on how the particle approaches the surface, as the particle-surface potential might have an energy barrier to access a certain adsorption site along the reaction coordinate. Indeed, this is the case for H interacting with the basal plane of graphite. In experiments of interaction of thermal energy hydrogen atoms with single crystal graphite, it was found that an H atom gets trapped in shallow sites ($E \sim 32$ meV [34]), while in other studies 2000 K H atoms become trapped in strong adsorption sites (chemisorption) [35]. Theoretical calculations seem to support this picture [36, 37], predicting that there is a small activation energy barrier for chemisorption. Because of the high kinetic energy involved, this type of interaction is not relevant but in very special astrophysical environments.

Finally, we mention developments in surface science that, although they emerged in another context, are relevant to this problem. According to the Eley-Rideal (ER) mechanism [38], the atom from the gas phase impinges on the atom adsorbed on the surface and reacts with it before becoming equilibrated with the surface. The two mechanisms, LH and ER, were not easily distinguished until recently, when advances in surface science techniques made it possible to measure the energy of the ejected reactant (expected to be non thermal in the ER case) or the cross section of the reaction (a small cross section of atomic dimensions would imply a head-on collision and therefore the ER mechanism).

A useful way to examine the Eley-Rideal mechanism is by first depositing D atoms and then measuring their abstraction by an impinging beam of H atoms, which leads to the formation of HD molecules. In experiments reported by Zecho et al. [35], D atoms with 2000 K of kinetic energy are deposited on a highly oriented pyrolitic graphite sample consisting of small (5 μm in size) platelets of oriented graphite planes. After the deposition, an H beam is introduced and the rate of the reaction product (HD) evolving from the surface is measured as a function of time. The rate follows an exponential decay as $\sim \exp(-\Sigma \Phi_H t)$ where Σ is the cross section for the abstraction reaction and Φ_H is the flux of H atoms. It is found that Σ is of the order of a few Å^2 indicating that the H atom reacts directly with the D atom it hits, without prior accommodation to the surface.

There is also another mechanism, called hot-atom, which is somehow in between the ones described above. In this reaction, the atom impinging on the surface maintains some of its kinetic energy (and/or gain some of the condensation energy) and uses this energy to sample the surface quickly. The atom suffers multiple collisions with the surface during the accommodation process and in each collision has a non-zero probability of reacting with other adsorbed atoms (adatoms). These mechanisms, that should be considered as limiting cases of a range of processes leading up to the reaction, have been observed mostly in the study of the interaction of hydrogen atoms with well characterized metal and semiconductor surfaces. Although theoretical calculations [39] suggest that the E-R reactivity increases as the H-metal bond strength decreases, indicating a preference for the hot-atom mechanism, it is not clear how those results can be extrapolated to other types of surfaces. In Sec. 7 we discuss the applicability of the different reaction mechanisms to the formation of H_2 on actual grains in the ISM.

4. Experiments

4.1. Experimental methods

In experiments designed to study processes occurring in the ISM, one has to mimic the conditions of the particular ISM environment that one wishes to study. Of the three major requirements for the study of the formation of molecular hydrogen on dust grain analogues in the diffuse and dense cloud medium - low (10 - 20 K) sample temperature, low background pressure (10^{-10} torr), and low impinging flux of reactants (hydrogen atoms), the hardest to meet is the third. As discussed above, the arrival rate of H atoms on a grain surface is $n_H v_H \sigma$. With the parameters used earlier, one obtains that the flux per unit area is $\sim 2.5 \times 10^6$ (atoms cm^{-2} sec^{-1}). Unfortunately, this type of flux is utterly impossible to obtain in laboratory experiments. For example, the background pressure of 10^{-10} torr already is equivalent to an arrival rate of 10^{11} (atoms cm^{-2} sec^{-1}). If experiments are done with high fluxes one must have a very fine temporal control of the exposure of the sample to the incident atoms, so that the exposure (or time during which the sample is exposed to a flux of impinging particles) is very short. The reason for this requirement is that ultimately we want to be in operational conditions of low coverage (that is, fraction of sample covered by hydrogen atoms); obviously, exposure and coverage are related by the sticking coefficient. In our experiments we placed great care in reducing the flux as low as possible. Since the dissociation source that produces atomic hydrogen from molecular hydrogen can be operated with high (80-90%) dissociation efficiency only in a narrow supply pressure range, in certain experiments, when we needed to deposit very few atoms, we used a low (5%) duty-cycle mechanical chopper.

The experiment is conducted in two steps. In the first one, the sample is exposed to hydrogen atoms for a given amount of time. Any molecule generated during this time is detected by a mass-discriminating detector. According to the scenario implied by the theory of Hollenbach and Salpeter, molecules would form at this time since the time it takes an atom to diffuse and reach another one is orders of magnitude less than the time during which the sample is irradiated. However, there exists the possibility that the molecules do not get ejected into the gas phase

after being formed. Furthermore, it is also possible that atoms do not have the high mobility envisioned by Hollenbach and Salpeter. To check for these two latter possibilities, a second experiment is done in which the sample temperature is rapidly raised and the products evolving from the surface are collected. This process is called thermal programmed desorption (TPD). It can be modeled using the Polanyi-Wigner equation

$$R(t) = \nu N(t)^m \exp(-E_d/k_B T) \tag{3}$$

where $R(t)$ is the rate of the atomic/molecular species departing the surface, $N(t)$ is the number density of atoms/molecules on the surface, ν is their vibration frequency within adsorption wells and E_d is the activation energy for desorption. Here, m is the order of the desorption process. For $m = 0$, the desorption rate does not depend on the number of atoms/molecules on the surface. This is the case when the surface is covered by at least several layers of the particles to be desorbed . For $m = 1$ the desorption rate is linearly proportional to the number density of the adsorbed species. For $m = 2$ the rate depends quadratically on the number density, as in the formula that we proposed to explain the second order desorption kinetics we observed for the experiment on the polycrystalline sample. This is of course a phenomenological equation, and its validity rests on a number of assumptions (see Ref. [40]), among which there is the independence of the desorption energy on coverage (and this is not too bad an approximation in our case, since we try to work at very low coverage, down to a few percent of a ML). The Polanyi-Wigner equation works reasonably well in order to obtain a preliminary understanding of the processes being investigated. However, to confirm the validity of its application and to obtain more specific information, we used a rate equation approach (discussed below) to analyze our data.

Fig. 1 shows an example of TPD performed on a polycrystalline olivine sample after the surface had been irradiated with H and D atoms at the temperature of 7 K (the reason to use deuterium atoms is explained below). One can easily note that in the lower panel, corresponding to the shortest irradiation times, the maximum in the desorption occurs at smaller temperature as the irradiation time, and consequently the coverage, is increased. This is a hallmark of second order desorption kinetics, and the observation of this has led us to propose Eq. (2). When the irradiation time is sufficiently long, but still below one layer of coverage as determined in other experiments, the position of the maximum does not shift anymore and the shape becomes more asymmetric, and these are signs of first order desorption.

4.2. The apparatus

In order to carry out the measurements described in the previous section, we have extensively modified an apparatus that was previously used for surface science experiments of interaction of atomic beams with well characterized crystalline surfaces. Although the apparatus has been described in detail previously, here we summarize its main features in the current configuration. The apparatus, located in the Physics Department of Syracuse University (Syracuse, NY- USA) consists of three sections (see Fig. 2): two atomic/molecular beam lines that can be operated independently, a sample and detector chamber, and a time-of-flight section. The last two sections are operated in ultra-high vacuum (UHV) conditions and reach routinely a background pressure in the 10^{-10} torr range.

The reason why two beam lines are used simultaneously, one with hydrogen and the other with deuterium supply gas, is threefold. First, even when there is good dissociation, about 10% of the molecular gas is not dissociated and therefore is sent to the sample along with the atomic gas. It would then be difficult to discriminate the formation of H_2 on the surface from this spurious contribution. Second, H_2 is the most abundant residual gas in a well cleaned and baked UHV chamber; this background gas would become adsorbed on the surface of the sample and it would be indistinguishable from the formation of H_2 occurring on the sample. Third, if
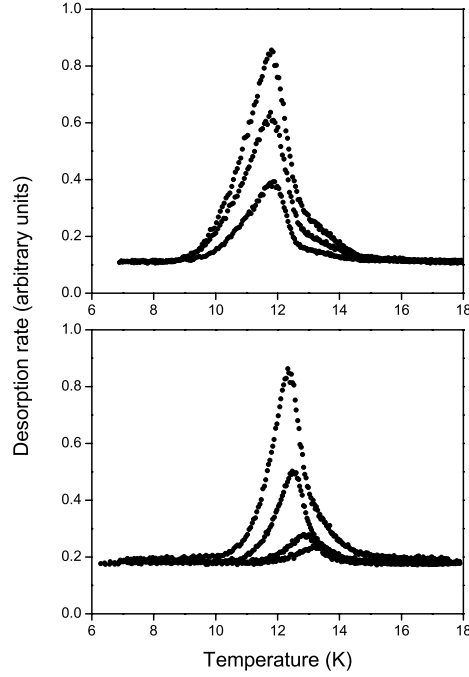
Figure 1. Desorption rate of HD during TPD runs from an olivine slab after irradiation at surface temperature of 6 K, for long irradiation times (top) of 2.0, 5.5 and 8.0 minutes and short irradiation times (bottom) of 0.07, 0.1, 0.25 and 0.55 minutes. The flux is of the order of 10^{12} atoms/cm^2/sec. See Ref. [21] for details

we use H atoms in one line and D atoms in the other, the only place where they can form HD is on the sample surface. The product molecule, HD, has mass 3 that is not typically present in a residual gas, and thus very small amounts of HD coming from the sample can be detected using a mass spectrometer.

The two beam lines consist each of three differentially pumped sections, a radiofrequency powered dissociation source and mechanical choppers for in-phase detection or time-of-flight characterization of the beams. Each source consists of a Pyrex tube ending with an aluminum nozzle that can be cooled to $\sim$ 200 K via a copper braid connected to a liquid nitrogen reservoir. Each source has a water cooled jacket and is surrounded by a cavity in which the radiofrequency is coupled to the gas inductively. For hydrogen and deuterium dissociation, a total RF power of about 100 Watts is used. Dissociation rates obtained are routinely in the 80-90% as measured using a mass-discriminating detector (a quadrupole mass spectrometer) located in the main chamber. The inlet pressure of molecular hydrogen is monitored by a Baracel or equivalent pressure cell and is regulated using fine metering valves.

The two beam lines are aimed at a target located in the main UHV chamber. The sample is mounted on a copper support which is then screwed onto a Heli-Trans continuous flow cold finger. The temperature of the sample can be changed by throttling the flow of liquid helium or by using a heater housed in a ceramic box fastened on the back of the thin vertical copper slab that holds the sample and a retaining ring. A silicon diode thermometer and a gold-iron/chromel thermocouple measure the temperature at the back of the sample. In a typical
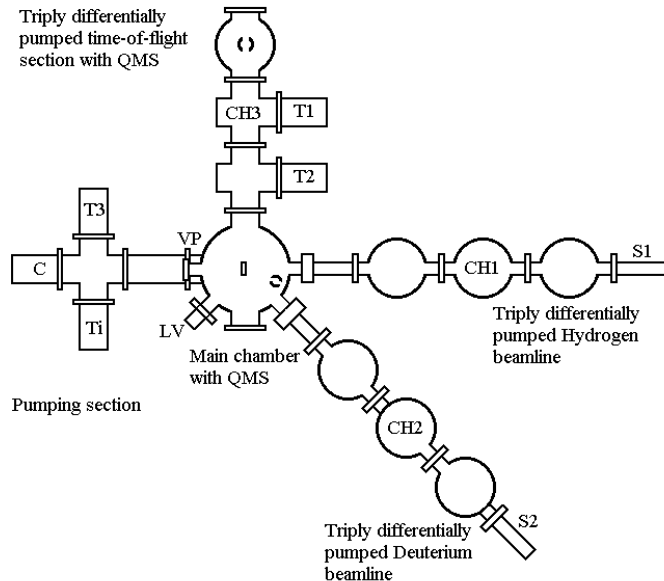
Figure 2. Schematic of the apparatus - top view. S1 and S2 denote H_2 and D_2 radio-frequency dissociation sources; CH1, CH2 and CH3 denote the positions of mechanical choppers; T1, T2 and T3 are turbopumps while Ti is a titanium sublimation pump and C a cryopump; LV is the leak valve for introducing water vapor into the system through a capillary. See Ref. [26] for details.

run, the temperature is held fixed between 4.5 and 30 K while the sample is exposed to the atomic/molecular beams. In a TPD experiment the flow of liquid helium is cut off and the temperature of the sample rises quickly and in a predictable manner. To clean the sample during a long set of measurements, the temperature is raised over 230 K to remove any water deposits by cutting the flow of liquid helium and using two heaters, the one located behind the sample and another mounted further up on the cold finger. To avoid contamination of the sample from background gas during measurements, a ultra-high vacuum environment is kept by using suitable materials with low outgassing rates and appropriate pumps. The main chamber is pumped by a turbopump, an ion pump and a cryopump which assure that when the sample or the cold finger temperature are suddenly raised for a TPD experiment, the gases evolving from the sample and its supports are quickly pumped away. In typical operating conditions, we observed little or negligible back-adsorption of these gases onto the sample.

The sample can be moved vertically to be positioned in front of the atomic/molecular beam lines or facing a capillary for water vapor deposition. The sample holder can also be rotated around its axis in order to face the beam lines or the time of flight section. To make sure that the atomic/molecular beams of about 3 mm diameter - hit the same spot on the sample simultaneously, two He-Ne lasers are placed at the back of the sources when the apparatus has been opened up to atmospheric pressure, and the sources and beam lines are adjusted until the two laser spots superimpose on the sample.

The detector, a quadrupole mass spectrometer, is housed in a differentially pumped enclosure with two apertures diametrically located to let the gas pass through. The detector can be rotated to measure the intensity of each of the beams; during the measurements of the reaction products it is placed between the beam lines. In order to measure the dissociation efficiency, the detector is positioned facing one of the line and is tuned to the molecular mass of the source gas, i.e. mass

2 for H_2 and mass 4 for D_2. The change in the detector signal with the dissociation on and off gives the degree of dissociation; this method of measurement avoids the problem of recalibrating the efficiency of the detector for different masses, for example if one wanted to measure the dissociation tuning the detector first on mass H_2 (dissociation off) and then on H (dissociation on).

The time-of-flight appendix consists of three differentially pumped chambers separated from each other by 5 mm diameter collimators. These collimators define a straight-line path from the sample, through the slots of a constant speed mechanical chopper wheel mounted in the second vacuum chamber, and through the ionizing region of a quadrupole mass spectrometer mounted in the third chamber. The slots of the chopper wheel break the flow of particles desorbing from the sample into pulses of particles that are admitted into the free-flight region between chopper wheel and detector. A LED/photodiode pair is used to detect a triggering slot or slots on the chopper wheel for synchronizing the detector with the wheel rotation.

The translational velocity distribution of gas particles within the pulses can be determined from the known chopper-detector distance and the flight times of particles across that distance. In the conventional method of time-of-flight detection, a chopper wheel with a set of equally spaced, narrow slots is used to admit pulses of gas into the free-flight region at a regular frequency. The number of slots and their angular width are chosen for a minimum of spatial overlap between successive pulses reaching the detector (with broadening effects such as the dispersion of each pulse over the free-flight distance taken into account). This method provides the advantage that the detector directly records the broadened time-of-flight distribution of the gas, but with the disadvantage that the open area of the slots is limited to a few percent of the area of the chopper wheel.

We have also implemented another method to measure the time of flight. The cross-correlation method of time-of-flight detection uses a chopper wheel with a pseudo-random pattern of slots to intentionally admit spatially overlapping pulses of gas into the free-flight distance. The detector integrates these pulses into an irregular waveform that only reproduces the time-of-flight distribution in the gas when the waveform is cross-correlated with the pseudo-random pattern of slots; the pseudo-random pattern of the slots is chosen for a near optimal transmission of the time-of-flight distribution through this process. An advantage of this method of time-of-flight detection over the conventional method is that the open area of the slots is nearly 50%, thus potentially allowing a great reduction in the amount of detection time required to achieve a given signal-to-noise ratio. Drawbacks of this method are stringent requirements for the rotational stability of the chopper motor and the precision with which the detector is synchronized with the motor, as well as the additional cross-correlation calculation needed to extract the time-of-flight distribution from the detector response.

5. Results

For our experiments of H_2 formation on dust grain analogues we looked at three classes of materials, each representing a different type of dust grain present in the ISM: silicates, carbonaceous particles, and ice-coated grains. For a discussion of different models of dust grains in the ISM, see [24].

As mentioned before, experiments to measure the recombination efficiency, defined as the probability that two atoms hitting the surface recombine, were done in two steps. In the first, while the sample is exposed to beams of H and D atoms, the HD molecules evolving from the surface are measured. This efficiency of HD formation turns out to be quite low, at most 10%, except at the lowest temperatures (< 10 K). Next, after the exposure is completed, the surface temperature is raised quickly (the TPD part of the experiment) and HD molecules coming off the sample are detected, see Fig. 1 for an example of the rate of desorption as a function of the temperature of the sample. Therefore, the trace is proportional to the number of HD molecules
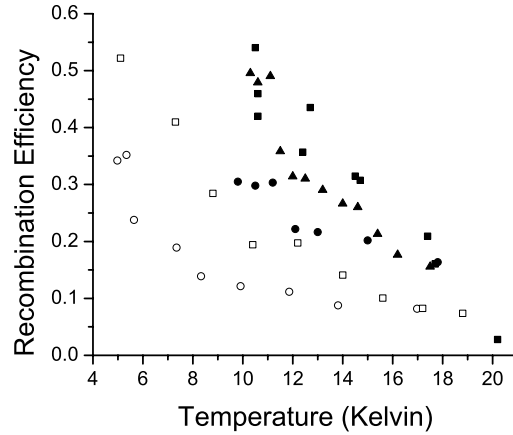
Figure 3. Recombination efficiency of molecular hydrogen vs. sample temperature of H atoms. Filled circles are for high density amorphous ice, open circles are for low density amorphous ice prepared by heating high density amorphous ice. Open squares are for water vapor-deposited low-density amorphous ice. The scatter in the data points reflects the variability in the ice preparation methods.

coming off the sample in a temperature interval dT. In order to obtain the recombination efficiency, the data have to be treated as follows. The background is subtracted out and a correction for the solid angle of the detector and the speed of the molecules going through the detector is applied to the value of the integrated trace. One then has to correct this number because some H (or D) atoms will form H_2 (or D_2) instead of HD; finally, the number so obtained is divided by the measured intensities of the H and D beams integrated over the time of the exposure. The experiment is then repeated for exposures at different sample temperatures, and a graph as shown in Fig. 3 is obtained. The exposure used for these experiments is the shortest that is possible while having a large enough signal/noise ratio for the analysis.

Fig. 4 shows typical traces of TPD for HD desorbing from water ice. It is known that there are several solid phases of water ice. In the ISM, the high density amorphous ice phase is the most abundant, but low density amorphous and crystalline phases have also been detected. Following the recipe of Jennisken et al. [41] who characterized water ice amorphous phases, the high density phase can be made by depositing water vapor on a cold substrate at low ($\sim$10 K) temperature. If the ice is warmed past 38 K, a gradual irreversible change occurs and the ice transforms in low density ice. Finally, at much higher temperature ($\sim$130 K, depending on the experimental conditions [42]) low density amorphous ice transforms in crystalline ice (alternatively, crystalline ice can be obtained by water vapor deposition at a temperature $T > 133$ K [43]). We followed the recipe of Jennisken and Blake in order to make the different types of amorphous ice, while "crystalline" ice was prepared by depositing water vapor at $133K$. Details on deposition methods and treatment are given in Refs. [25, 26]. The important point is that the three different ices give different TPD traces (because there is no annealing of these samples, traces might change slightly from time to time. Consequently, the shape or relative heights or widths of features in the TPD traces might change, but overall we observed the same type of feature during the course of our investigations).

We mentioned previously that there are different possible routes for the formation of molecular hydrogen on the surface of a dust grain. H_2 could form immediately by the Eley-Rideal process
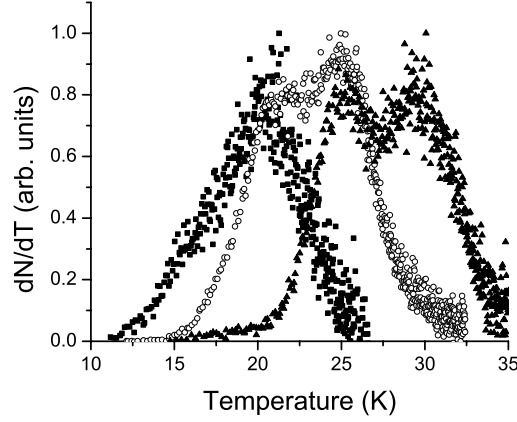
Figure 4. Desorption rate of HD as a function of temperature after adsorption of H and D at ∼10K. From left to right: desorption from crystalline ice, low-density amorphous ice and high-density amorphous ice. The height of the traces has been normalized for ease of comparison. See Ref. [44] for more details.

in which an H atom from the gas-phase reacts with one on the surface. This is unlikely the case here, since the coverage is low and little H_2 is detected coming off the surface during the irradiation phase. Then there is the case of a quick reaction between two H atoms that have landed on the surface and moved rapidly due to diffusion by tunneling. In our experiment, we would expect that the HD molecule just formed on the surface would be ejected out because of the energy released in the reaction, and again we measure a very small signal due to ejection of HD during the irradiation phase. However, it might be the case that the HD molecule is successful in becoming thermalized with the surface; in this case it would remain on the surface. The reason why this could happen is that in a porous solid as amorphous water ice it is possible for the nascent molecule to make enough collisions to get thermalized without getting ejected. In order to understand if this is the case and the mechanisms of reaction, we did an experiment in which we deposited HD molecules on the surface of ice under the same conditions as when we deposited H and D atoms. We did then a TPD and compared the two traces. If HD formed on the surface and stayed, then the two traces, one obtained placing HD on the surface and the other exposing the surface to H and D atoms, would be identical. But, as one can see from Fig. 5, they are different, indicating that in the experiment in which the surface is exposed to H and D atoms, the TPD experiment causes the atoms to migrate, form molecules which are then expelled. The diffusion and desorption processes of atomic hydrogen on the surface are controlled by different energy barriers than the desorption of hydrogen molecules that were deposited on the surface. In order to obtain quantitative information, Perets et al. have used a rate equation model that we describe in detail below [45].

To determine the distribution of kinetic energies of hydrogen molecules forming and desorbing from the sample surface, we exposed the sample to H and D atoms and then ramped the sample temperature for a TPD with the sample surface rotated to face the time-of-flight line. In Fig. 6 we show a time-of-flight spectrum of HD molecules desorbing from a high-density ice layer. The ice layer was exposed to the H and D beams for 90 minutes at layer temperature of 8 K. Also shown are time-of-flight spectra of D_2 molecules desorbing from a high-density ice layer. In one spectrum the sample temperature was 7 K when it was exposed to the beam of D atoms for 40 minutes. In the other spectrum the sample was exposed to a beam of D_2 molecules. A
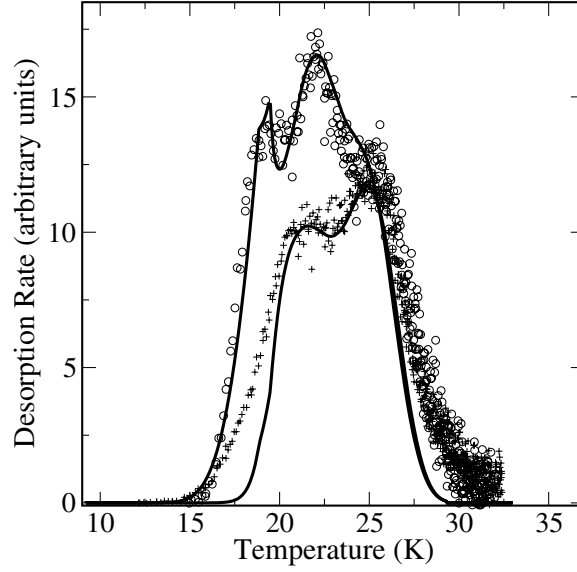
Figure 5. TPD curves of HD desorption after irradiation with HD molecules (○) and H+D atoms (+) on low density ice. The solid lines are fits obtained by the rate equations model. See Ref. [45] for more details.

200 Hz chopper motor was used in these three measurements; Each of the three time-of-flight traces in Fig. 6 was fitted with a distribution of flight times based upon a Maxwell-Boltzmann distribution of velocities for the particles desorbing from the sample. For an effusive flow of particles of mass m and temperature T desorbing from the sample, the number density $n(t)$ of particles with flight times between t and $t + dt$ is given by

$$n(t)dt \sim f(t)dt \sim \frac{1}{t^4} \exp\left(\frac{-mL^2}{2k_B T t^2}\right), \tag{4}$$

where L is the chopper to detector flight distance. Experimentally, each time-of-flight spectrum will also be broadened due to effects such as the finite size of the chopper slits or the finite cross-sectional diameter of the collimating holes [46]. The function $f(t)$ was convoluted with a suitable broadening function to take these effects into account before being used to fit the time-of-flight spectra in Fig. 6. The kinetic temperature associated with each spectrum can be derived from the maximum value of $f(t)$:

$$T_{\text{kin}} = \frac{mL^2}{4k_B t_{\text{peak}}^2}. \tag{5}$$

The kinetic temperatures for the time-of-flight spectra in Fig. 6 are 24 K for the desorbing HD molecules and 25 K for both spectra of desorbing D_2 molecules. For all three of the time-of-flight spectra in Fig. 6, the kinetic temperature of the desorbing molecules are roughly similar to the temperature at which the desorption rate of that molecule is a maximum. A scenario that can explain these results is that a molecule desorbing from an irregular amorphous ice surface might be more likely to make one or more collisions with the ice surface.
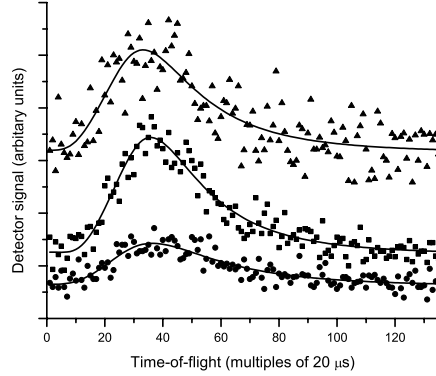
Figure 6. Time-of-flight traces of HD and D_2 desorbing from high-density amorphous ice. Shown are the sum of two HD spectra taken after 90 minutes of H and D exposure at a sample temperature of 8 K (closed triangles), a D_2 spectrum taken after 40 minutes of D_2 exposure at 7 K (closed squares), and a D_2 spectrum taken after 40 minutes of D exposure at 7 K (closed circles). Solid lines are curve fits with a Maxwell-Boltzmann function convoluted with a broadening function to correct for instrumental effects. See Ref. [27] for more details.

Hornekaer et al. [28, 47] have used the laser-induced thermal desorption (LITD) technique to investigate the time-of-flight distribution of the thermal desorption of HD molecules forming from H and D exposure of a vacuum-deposited amorphous water ice layer (which they denote amorphous solid water or ASW). The LITD technique involves using a laser pulse to rapidly heat the sample surface on time scales short compared to those for thermal desorption of the adsorbed species (see Ref. [48] for a detailed description). Hornekaer et al. reported a peak temperature of 45 ± 10 K for the temperature of their ASW ice layer when heated by a laser pulse and measured time-of-flight distributions for HD and D_2 desorbing from the sample consistent with a 45 K Maxwell-Boltzmann distribution of velocities. This group's measurements are an independent determination that the kinetic energy from H and D recombinations on an amorphous ice surface is lost to the ice layer before the newly formed HD molecules desorb.

6. Analysis

In our TPD experiments most of the adsorbed hydrogen is released well before a temperature of 30K is reached. This indicates that the hydrogen atoms on the surface are trapped in physisorption potential wells and are thus only weakly adsorbed. We also assume that the mechanism for the creation of H_2 (or HD) is the LH scheme, namely that the rate of creation of H_2 is diffusion limited [20].

In order to keep the number of parameters at a tractable level, we do not treat the two populations of H and D adatoms separately. Instead, we consider only one population of hydrogen atoms to which we refer as H adatoms. With this approach, the diffusion, reaction and desorption processes are controlled by the activation energy barriers for diffusion and desorption of H adatoms as well as the activation energy barrier for desorption of hydrogen molecules. In addition, we assume that among the molecules that form on the surface, some remain adsorbed, while the rest desorb upon formation. Such immediate desorption is possible in case that the 4.5 eV of binding energy of the H_2 molecule is not transformed efficiently into the substrate.

6.1. Experiments on olivine and amorphous carbon surfaces

Consider an experiment in which a flux of H atoms is irradiated on the surface and a large fraction of them stick. Once the surface temperature is raised, the adsorbed H atoms hop like random walkers between adsorption sites on the surface. When two H atoms encounter one another they may form an H_2 molecule. Let $N_H(t)$ [in monolayers (ML)] be the coverage of H atoms on the surface and $N_{H_2}(t)$ (also in ML) the coverage of H_2 molecules. We obtain the following set of rate equations:

$$\dot{N_H} = F(1 - N_H - N_{H_2}) - W_H N_H - 2\alpha N_H^2 \tag{6a}$$
$$\dot{N_{H_2}} = \mu\alpha N_H^2 - W_{H_2} N_{H_2}. \tag{6b}$$

The first term on the right hand side of Eq. (6a) represents the incoming flux in the LH kinetics. In this scheme H atoms deposited on top of H atoms or H_2 molecules already on the surface are rejected. F represents an *effective* flux (in units of ML/sec), namely it already includes the possibility of a temperature dependent sticking coefficient. The second term in Eq. (6a) represents the desorption of H atoms from the surface. The desorption coefficient is

$$W_H = \nu \exp(-E_H^{des}/k_B T), \tag{7}$$

where ν is the vibration frequency (standardly taken to be 10^{12} s^{-1}), E_H^{des} is the activation energy barrier for desorption of an H atom and T is the surface temperature. The third term in Eq. (6a) accounts for the depletion of the H population on the surface due to recombination into H_2 molecules, where

$$\alpha = \nu \exp(-E_H^{diff}/k_B T) \tag{8}$$

is the hopping rate of H atoms on the surface and E_H^{diff} is the activation energy barrier for H diffusion. The first term on the right hand side of Eq. (6b) represents the creation of H_2 molecules. The factor 2 in the third term of Eq. (6a) does not appear here since it takes two H atoms to form one molecule. The parameter $0 \leq \mu \leq 1$ represents the fraction of H_2 molecules that remain adsorbed on the surface upon formation, while the rest spontaneously desorb due to the excess energy released in the recombination process. The second term in Eq. (6b) describes the desorption of H_2 molecules. The desorption coefficient for H_2 molecules is

$$W_{H_2} = \nu \exp(-E_{H_2}^{des}/k_B T), \tag{9}$$

where $E_{H_2}^{des}$ is the activation energy barrier for H_2 desorption. The production rate R of H_2 molecules is given by:

$$R = (1-\mu)\alpha N_H^2 + W_{H_2} N_{H_2}. \tag{10}$$

This model can be considered as a generalization of the Polanyi-Wigner model. It gives rise to a wider range of simultaneous applications and describes both first order and second order desorption kinetics (or a combination) for different regimes of temperature and flux.

In the experiments analyzed here, both the temperature and the flux were controlled and monitored throughout. Each experiment consists of two phases. In the first phase the sample temperature is constant up to time t_0, under a constant irradiation rate F_0. In the second phase, the irradiation is turned off and an approximately linear heating of the sample is applied at the average rate b (K/sec):

$$F(t) = F_0; \quad T(t) = T_0 : \qquad 0 \leq t < t_0 \tag{11a}$$
$$F(t) = 0; \quad T(t) = T_0 + b(t - t_0) : \quad t \geq t_0. \tag{11b}$$

Here T_0 is the constant temperature of the sample during irradiation.

In order to extract the parameters that are relevant to the diffusion, reaction and desorption processes of H atoms on the samples we performed numerical integration of Eq. (6). The numerically generated TPD curves were fitted to the experimental ones by varying the parameters E_H^{diff}, E_H^{des}, $E_{H_2}^{des}$ and μ until the best fit was obtained. The parameters that gave rise to the best fits were $E_0 = 24.7$, $E_1 = 32.1$, $E_2 = 27.1$ (meV) and $\mu = 0.33$ for olivine, and $E_0 = 44.0$, $E_1 = 56.7$, $E_2 = 46.7$ (meV) and $\mu = 0.41$ for amorphous carbon.

Due to the Langmuir rejection mechanism, the coverage of H atoms on the surface, $N_H(t)$, does not grow linearly with the irradiation time, t, but is given by

$$N_H(t) = 1 - \exp(-F_0 t). \qquad (12)$$

Using this feature we obtained the density of adsorption sites on the surface. To this end, the flux densities of the H and D beams were measured directly. The total yield of HD molecules was then fitted to Eq. (12), which enabled us to evaluate the flux F_0 in ML/sec for each sample. We obtained $F_0 = 2.7 \cdot 10^{-4}$ (in ML/sec) for the olivine experiment and $F_0 = 9.87 \cdot 10^{-4}$ for the amorphous carbon experiment. From these results we found that the density of adsorption sites on the olivine surface is $s \cong 2 \cdot 10^{14}$ and for the amorphous carbon surface $s \cong 5 \cdot 10^{13}$ (sites cm^{-2}).

6.2. Experiments on ice surfaces

The analysis of the hydrogen recombination experiments is complicated because they involve a combination of diffusion of atoms and molecules, reaction and desorption processes. Additional information can be obtained by the analysis of experiments that involve only molecules, in which there are no reaction processes and the results are dominated by molecular desorption. In these experiments a given amount of molecular hydrogen is irradiated on the surface, followed by a TPD run. From the results one can obtain the distribution of energy barriers for desorption of hydrogen molecules from the surface. These parameters can then be used in the analysis of experiments on hydrogen recombination, reducing the number of fitting parameters used in their analysis.

TPD experiments with irradiation of molecules were recently performed on amorphous ice surfaces [26, 45, 47]. The TPD curve obtained after irradiation by HD molecules on low density ice (LDI) is shown in Fig. 5 (circles). To fit these TPD curves one needs to assume a broad distribution of energy barriers for desorption of hydrogen molecules. Furthermore, for low density ice, the TPD curves are best fitted by a model that includes three types of adsorption sites for molecules with different energy barriers for desorption. Below we present a model that provides a good description of all the experiments on ice, those with irradiation of atoms as well as those with irradiation of molecules. In the model we assume a given density of adsorption sites on the surface. Each site can adsorb either an H atom or an H$_2$ molecule. In terms of the adsorption of H atoms, all the adsorption sites are assumed to be identical, where the energy barrier for H diffusion is E_H^{diff} and the barrier for desorption is E_H^{des}. As for the adsorption of H$_2$ molecules, we assume that the adsorption sites may differ from each other. In particular, we assume that the population of adsorption sites is divided into three types. A fraction μ_j of the sites belong to type j, where $j = 1, \ldots, 3$, and $\sum_j \mu_j = 1$. The energy barrier for desorption of H$_2$ molecules from an adsorption site of type j is $E_{H_2}^{des}(j)$.

Let N_H [in monolayers (ML)] be the coverage of H atoms on the surface. Similarly, let $N_{H_2}(j)$ (also in ML) be the coverage of H$_2$ molecules that are trapped in adsorption sites of type j. Clearly, this coverage is limited by the number of sites of type j and therefore $N_{H_2}(j) \leq \mu_j$. The total coverage of H$_2$ molecules is given by $N_{H_2} = \sum_{j=1}^{3} N_{H_2}(j)$. Since we assume that each site can host only one atom or one molecule, the coverage does not exceed a monolayer, and thus $N_H + N_{H_2} \leq 1$. For the case of LDI we thus obtain the following set of rate equations

$$\dot{N}_{\mathrm{H}} \quad = F\left(1 - N_{\mathrm{H}} - N_{\mathrm{H}_2}\right) - W_{\mathrm{H}}N_{\mathrm{H}} - 2\alpha N_{\mathrm{H}}^2 \tag{13a}$$

$$\dot{N}_{\mathrm{H}_2}(1) \quad = \mu_1 \alpha N_{\mathrm{H}}{}^2 - W_{\mathrm{H}_2}(1)N_{\mathrm{H}_2}(1) \tag{13b}$$

$$\dot{N}_{\mathrm{H}_2}(2) \quad = \mu_2 \alpha N_{\mathrm{H}}{}^2 - W_{\mathrm{H}_2}(2)N_{\mathrm{H}_2}(2) \tag{13c}$$

$$\dot{N}_{\mathrm{H}_2}(3) \quad = \mu_3 \alpha N_{\mathrm{H}}{}^2 - W_{\mathrm{H}_2}(3)N_{\mathrm{H}_2}(3). \tag{13d}$$

Eq. (13a) is identical to Eq. (6a). Eqs. (13b)-(13d) describe the population of molecules on the surface. The first term on the right hand side of each of these three equations represents the formation of H_2 molecules that become adsorbed in a site of type $j = 1$, 2 or 3. The second term in Eqs. (13b)-(13d) describes the desorption of H_2 molecules from sites of type j, where

$$W_{\mathrm{H}_2}(j) = \nu \exp(-E_{\mathrm{H}_2}^{\mathrm{des}}(j)/k_B T) \tag{14}$$

is the H_2 desorption coefficient and $E_{\mathrm{H}_2}^{\mathrm{des}}(j)$ is the activation energy barrier for H_2 desorption from an adsorption site of type j. The H_2 production rate R is given by:

$$R = \sum_{j=1}^{3} W_{\mathrm{H}_2}(j)N_{\mathrm{H}_2}(j). \tag{15}$$

The main difference between this model and the model used previously in the analysis of the olivine and carbon experiments is in the way molecules desorb from the surface. In the earlier model, a fraction $1 - \mu$ of the molecules, desorb from the surface upon formation. This was interpreted as a result of the 4.5 eV of binding energy which is not transferred efficiently into internal degrees of freedom of the grain. In the model used for the ice experiments, hydrogen molecules do not desorb upon formation but become trapped in adsorption sites. This requires an efficient transfer of the the bidning energy into the grain. On porous surfaces, repeated collisions of the molecule with the surface are possible, which may help to transfer the energy to the grain.

The model used for the analysis of the ice experiments is motivated by the results of the experiments with irradiation by molecules shown in Fig. 5. The TPD curve of HD desorption obtained after irradiation with H and D atoms is also shown in Fig. 5. A comparison between the TPD curves obtained after irradiation by HD molecules and those obtained after irradiation by H and D atoms on LDI provides strong evidence for the proposed model. In experiments with irradiation of hydrogen atoms, the TPD curve consists of two peaks. These peaks coincide with the two higher peaks, among the three that are obtained after irradiation with molecules. The lowest peak is wiped out. This is because in the experiments in which atoms are irradiated, molecules are formed only at a later stage, after the temperature has been raised. At that time, the binding energy at the sites that correspond to the lowest peak is already insufficient for binding hydrogen molecules.

6.3. Astrophysical implications

Although the experiments that are described below were done with a very low flux of hydrogen atoms, the laboratory flux is still orders of magnitude higher than the one impinging on an actual dust grain in the ISM. Therefore, it is necessary to use theoretical tools in order to extract from experimental data information pertinent to the ISM. We do the following. First, once a preliminary analysis of the data has individuated the main physical processes at play, the theoretical model is built and the parameters are obtained from a fit to the data. Then, once it has been verified that the model is viable, the theory, using the parameters coming from the experiments, can be used to predict the results of processes that are actually happening in the
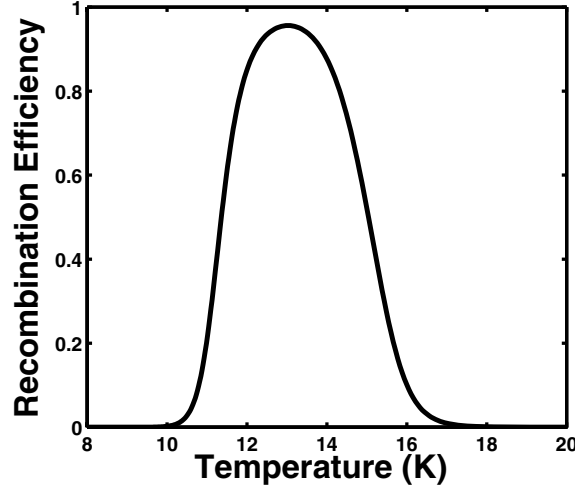
Figure 7. Recombination efficiency of molecular hydrogen formation on LDI vs. surface temperature. High efficiency is obtained in the temperature range between 11-16 K. See Ref. [45] for more details.

ISM. Katz et al. used rate equations to fit the data of hydrogen recombination on amorphous carbon and polycrystalline olivine [49]. The activation energy barriers for the relevant diffusion and desorption processes were extracted from the data. These barriers were used in order to calculate the efficiency of recombination for a range of low fluxes of hydrogen atoms and grain temperatures which are typical in the interstellar space [49].

The experimental results indicate that the mobility of H atoms on the surface is dominated by thermal hopping rather than tunneling. To examine the astrophysical implications of the results we used the rate equations to calculate the formation rate of H_2 under conditions that are typical in diffuse clouds. In Fig. 7 we present the recombination efficiency of H_2 molecules vs. surface temperature for LDI with 5×10^{13} adsorption sites per cm², exposed to a flux of H atoms from the gas phase, with density of $n_H = 10$ (cm^{-3}) and gas temperature ofn 100 K. This calculation, for the ice surface was done using Eq. (13).

It turns out that the temperature range in which H atoms are highly mobile on the surface but resides on it long enough to find each other and recombine is rather narrow. For ice, it is between 11 K and 16 K. At higher temperatures atoms desorb from the surface before they have sufficient time to encounter each other. At lower temperatures diffusion is suppressed while the Langmuir rejection leads to saturation of the surface with immobile H atoms and recombination is suppressed.

In general, the temperature range in which H_2 formation is highly efficient is given by

$$\frac{E_H^{\text{diff}}}{k_{\text{B}} \ln(\nu/F)} < T < \frac{2E_H^{\text{des}} - E_H^{\text{diff}}}{k_{\text{B}} \ln(\nu/F)}. \tag{16}$$

The width of this range is thus proportional to the difference between the diffusion and desorption barriers of H atoms on the surface. For the olivine sample, under typical flux that exists in diffuse clouds, the temperature window of high efficiency was found to be in the range $8 < T < 12$ (K), while for amorphous carbon it is $12 < T < 16$ (K).

7. Discussion

7.1. Molecular hydrogen formation in photon-dominated regions

The results of the laboratory experiments indicate that a combination silicate and carbon grains may serve as efficient catalysts for H_2 formation in diffuse and dense molecular clouds. Given the fact that there must be some mobility of H atoms on surfaces of grains in the temperature range 10 to 20 K, the binding of H on grains must be governed by weak physisorption forces. However, molecular hydrogen has also been observed in photon-dominated regions (PDR's), where the temperature of dust grains is typically between 30-50 K [50, 9]. These high temperatures are caused by far untraviolet photons, which penetrate into the interstellar clouds and heat the gas and dust in these regions. In particular, dust grains are heated through photoelectric heating while H_2 molecules are heated through photon absorption. The surface recombination processes observed in the laboratory experiments cannot produce molecular hydrogen at these high surface temperatures. At these temperatures, the residence time of hydrogen atoms in physisorption sites on the surface is too short for recombination to take place.

In order to explain the existence of molecular hydrogen in PDR's, Hollenbach and Salpeter [4] suggested that the grain surfaces contain enhanced adsorption sites with "semi-chemical binding", where atoms can stick much stronger. As a result, these atoms stay longer on the surface, allowing more time for pairs of hydrogen atoms to recombine before they desorb. For carbon materials, it was shown that these enhanced binding sites can be chemisorption sites, and their binding energies were calculated [51, 52, 53, 54].

According to recent analysis, the chemisorption model predicts high recombination efficiency at PDR temperatures, given that the energy barriers for entering the chemisorption sites are not larger than the binding energies of the physisorption sites, i.e., ~ 50 meV [56, 9]. However, ab initio calculations show that the energy barrier for an H atom to enter a chemisorption site on a graphite surface is $\simeq 0.2$ eV [36, 57, 58]. Such barriers prevent H atoms from entering chemisorption sites at grain temperatures lower than 100 K. These results were confirmed by recent experiments in which an activation energy barrier of 0.18 eV was found for hydrogen on C(0001), [59]. If such barriers exist also on the amorphous surfaces of interstellar dust grains, chemisorption sites are not likely to play a major role in H_2 formation on dust grains in PDR's.

7.2. The role of chemisorption sites

The experiments of H_2 formation on amorphous carbon and polished olivine have also been analysed by Cazaux and Tielens [55, 56] using a different, more complex model. They introduced additional free parameters with respect to the Katz et. al. model and also extended their analysis to the formation of H_2 at much higher temperatures. The differences between this model and the Katz et. al. model are as follows. First, Cazaux and Tielens take into account the presence of both physisorbed *and* chemisorbed sites on the surface. Second, their model allows quantum mechanical diffusion in addition to the thermal hopping of absorbed H atoms. Third, they treat separately the H and D isotopes used in the experiments. Using this model Cazaux and Tielens fitted the experimental TPD curves obtained in the polycrystalline olivine and amorphous carbon experiments. They found that quantum mechanical tunneling between physisorption sites is too slow to be important, supporting the Katz et. al. model. Their analysis suggested that it may be important (under certain assumptions on the energy barriers between physisorption and chemisorption sites) to populate chemisorption sites at low temperatures. Results similar to the ones in Katz et. al. were obtained for the energy barriers of the physisorbed sites. Additional experiments at much higher temperatures on a graphite surface [35] were used in order to obtain information on the energy barriers for the chemisorption sites. However, the results of the high temperature experiments are not fitted well using this model. This may indicate the possibility that additional processes take place under these conditions.

Other parameters of the Cazaux and Tielens' model have been only partially constrained

by the experimental data. Specifically, Cazaux and Tielens showed that chemisorption sites could have an important role in H_2 formation at low temperatures only if the energy barrier for entering a chemisorption site is much lower than expected by theory and found in recent experiments [36, 37, 35].

Thus, the chemisorption and tunneling processes suggested in this model do not seem to play an important role in the current experiments and in the conditions relevant for diffuse interstellar clouds and in PDRs. Differences in the behavior of H and D isotopes and their consequences that are considered in the model may be important, but need experimental evidence, which cannot be extracted from current experiments where measurements of H_2 and D_2 production have not been done.

7.3. Recent experiments by Hornekaer et al. on ice surfaces

Recently, Hornekaer et al. [28] presented interesting results on H+D recombination on porous and non-porous amorphous solid water (ASW). Amorphous ice is considered a good analog for ice mantles on grains in dark clouds. Their experiments were performed under conditions and using an equipment not too different from the one used by our group. Their atom beam fluxes were $\sim 10^{13}$ (atoms cm^{-2} sec^{-1}, namely about one order of magnitude higher than the fluxes used in our experiments. The range of exposure times was comparable. Hornekaer et al. investigated the kinetics of HD formation and measured the efficiency of recombination and the energetics of the molecules released from the ice layer after formation. The efficiency values they obtained are close to those obtained by our group on amorphous ice. The energy distribution of molecules formed showed that at least in porous amorphous ice, molecules are thermalized by collisions with the walls of pores (where they are formed) before they emerge into the gas phase.

Hornekaer et al. performed TPD experiments in which they irradiated H and D atoms either simultaneously or sequentially after waiting a delay time interval before dosing the other isotope. On porous ASW the results they obtained are consistent with a recombination occurring quickly after atom dosing due to a high mobility of the adsorbed atoms even at temperature as low as 8 K. This high mobility was attributed either to quantum mechanical diffusion or to the so called hot atom mechanism, where thermal activation is not likely to play a significant role at this temperature. This conclusion is sensible in light of the high coverages of H and D atoms irradiated in these experiments, which required the adsorbed atoms to diffuse only short distances before encountering each other. As already suggested in [16, 60], the hot atom mechanism may be able to provide the required mobility. In this case H and D atoms retain a good fraction of their gas phase kinetic energy during the accommodation process [61, 30]. This enables them to travel on the ice surface and inside its pores for several tens of Angstroms exploring several adsorption sites and recombining upon encountering already adsorbed atoms.

The reconciliation of their results with ours, which were obtained with low fluxes of atoms and short irradiation times, and hence at low coverages, comes from the fact that in our conditions the number of sites explored (which should be the same as in Hornekaer et al.'s experiment) by the hot atom during accommodation is not sufficient for this atom to encounter an already adsorbed atom and react with it with a significant probability. Indeed, this is confirmed quantitatively by a preliminary analysis (to be published in a forthcoming paper) of the irradiation process, using rate equations, in which the probability of reaction to form H_2 is proportional to the region of surface spanned by the hot atom. The solution of these equations, i.e. the number of H_2 molecules produced as a function of time during the adsorption phase, shows that under Hornekaer et al.'s conditions, H_2 molecules are readily formed, while in ours they are not. Therefore, in Hornekaer et al.'s case, all of the H_2 is formed by hot atoms making a few hops and encountering other previously adsorbed atoms. As observed experimentally by Hornekaer et al., the molecules remain trapped in the ice until the TPD is initiated. In our experiment, the atoms are too far apart from each other during the deposition phase, and the theoretical

analysis confirms our original interpretation [26] for H_2 formation on ice, and [20, 21, 49] for H_2 formation on olivine and amorphous carbon that atoms remain confined to their sites until the TPD is initiated.

7.4. The effect of grain size on H_2 formation efficiency

Rate equations are an ideal tool for the simulation of surface reactions, due to their simplicity and high computational efficiency. In particular, they account correctly for the temperature dependence of the reaction rates. However, the formation of molecular hydrogen in the interstellar medium takes place on grains of sub-micron size, under extremely low flux. In this case rate equations may not be suitable because they ignore the fluctuations as well as the discrete nature of the population of H atoms on each grain [62, 63, 64, 65]. For example, as the number of H atoms on a grain fluctuates in the range of 0, 1 or 2, the H_2 formation rate cannot be obtained from the average number alone. Recently, a master equation approach was proposed, that takes into account both the discrete nature of the population of H atoms as well as the fluctuations, and is thus suitable for the simulation of H_2 formation on interstellar dust grains [66, 67]. Since interstellar dust grains exhibits a broad distribution of sizes covering much of the range between a micron and a nano-meter, it is important to take the effect of grain size into account. However, the parameters obtained from the experiments, using rate equation analysis remain valid. Inserting these parameters into the master equation is expected to provide reliable results for the production rate of molecular hydrogen in interstellar clouds.

8. Summary

For more than a quarter of a century, the model of Hollenbach and Salpeter has stood as the reference point for the description of the molecular hydrogen formation on dust grain surfaces. Our experiments, the results of which were first published in 1997 [20, 21], showed that for certain models of grains the efficiency of recombination was below expectations; that a high recombination efficiency was obtained only within a narrow range of temperature of the grain; and that the kinetics of reaction hinted to hitherto neglected processes of mobility of H atoms on surfaces. Subsequent experiments on amorphous surfaces (amorphous carbon grains and two different phases of amorphous water ice) gave higher efficiency of recombination and over a wider temperature range, suggesting the possibility that morphology plays a substantial part. It also became clear that weak physisorption forces were responsible for the interaction of H atoms with the surface. In the meantime, theoretical work showed that the Hollenbach and Salpeter model and our model could both be responsible for the molecular hydrogen production, but under different ISM conditions [22]. In the last couple of years, other experimental and theoretical groups became interested in this problem. The work of Hornekaer et al. [28] confirmed our findings on the formation efficiency of H_2 on amorphous water ice and on the energetics of ejection, although their interpretation of their results (fast formation of molecules via athermal mechanisms) seemed at first sight to be at odds with our analysis of our data (H diffusion is initiated by thermal activation). We have shown in this paper that the different interpretations stem from the fact that the two experiments were done with fluxes differing by more than one order of magnitude. Specifically, the higher flux in the Hornekaer et al. experiments may have caused certain mechanisms, such as the hot atom mechanism, to become prominent and yield the rapid formation of molecules, while in our case the leading initiator of reactions is the thermally activated mobility. The theoretical work of Cazaux and Tielens [56] extended existing models to the case in which chemisorption sites are present on the surface, while confirming that at the low temperatures relevant to grains in quiescent diffuse and dense clouds, the laboratory results could be explained using physisorption forces and thermally activated diffusion. Recent progress in probing the mechanisms of formation of molecules on surfaces at higher temperatures [35] further improve the understanding of H_2 formation in a wider range of ISM conditions.

9. Acknowledgments

References

[1] Herbst E 2001 *Chem. Soc. Rev.* **30** 168
[2] Gould R J and Salpeter E E 1963 *Astrphys. J.* **53** 79
[3] Hollenbach D and Salpeter E E 1970 *J. Chem. Phys.* **53** 79
[4] Hollenbach D and Salpeter E E 1971 *Astrphys. J.* **163** 155
[5] Hollenbach D, Werner M W and Salpeter E E 1971 *Astrphys. J.* **163** 165
[6] Duley W W and Williams W A *Interstellar Chemistry* 1984 (New York: Academic Press)
[7] Jura M 1975 *Astrphys. J.* **197** 575
[8] Gry C, Boulanger F, Nehmé C, Pineau des Forets G, Habart E and Falgarone E 2002 *Astron. Astrophys.* **391** 675
[9] Habart E, Boulanger F, Verstraete L, Walmsley C M and Pineau des Forets G 2004 *Astron. Astrophys* **414** 531
[10] Smoluchowski R 1981 *Astrophys. and Space Sci.* **75** 353
[11] Smoluchowski R 1983 *J. Phys. Chem.* **87** 4229
[12] Brown L, Augustyniak W M, Simmons E, Marcantonio K J, Lanzerotti L J, Johnon R E, Boring J. W., Reimann C T, Foti G and Pirronello V 1982 *Nucl. Instr. Methods* **198** 1
[13] Pirronello V and Averna D 1988 *Astron. Astrophys.* **201** 196
[14] Averna D and Pirronello V 1991 *Astron. Astrophys.* **245** 239
[15] Pirronello V, Biham O, Manicó G, Roser J E and Vidali G 2000 in H$_2$ *in Space* Edited by: Combes F and Pineau des Forets G (Cambridge University Press) p. 71
[16] Pirronello V, Manico G, Roser J E and Vidali G 2004 in *Astrophysics of Dust*, Edited by Witt A et al., (ASP Series, Sheridan Books Ann Arbor, MI, USA) p. 529
[17] Darine B 1978 *Astrophys. J. Suppl.* **36** 595
[18] Draine B T 2003 *Annu. Rev. Astron. Astrophys.* **41** 241
[19] Colangeli L et al. 2003 *Astron. and Astrophys. Rev.* **11** 97
[20] Pirronello V, Liu C, Shen L and Vidali G 1997 *Astrphys. J.* **475** L69
[21] Pirronello V, Biham O, Liu C, Shen L and Vidali G 1997 *Astrphys. J.* **483** L131
[22] Biham O, Furman I, Katz N, Pirronello V and Vidali G 1998 *Mon. Notices Roy. Astron. Soc.* **296** 869
[23] Pirronello V, Liu C, Roser J E and Vidali G 1999 *Astron. Astrophys* **344** 681
[24] Mathis J 1966 *Astrophys. J.* **472** 643
[25] Manico G, Raguni, G, Pirronello V, Roser J E, Vidali G 2001 *Astrphys. J.* **548** L253
[26] Roser J E, Manicò G, Pirronello V and Vidali G 2002 *Astrophys. J.* **581** 276
[27] Roser J E, Swords S, Vidali G, Manico G and Pirronello V 2003 *Astrphys. J.* **596** L55
[28] Hornekaer L, Baurichter A, Petrunin V V, Field D and Luntz A C 2003 *Science* **302** 1943
[29] Perry J S A, Gingell J M, Newson K A, To J, Watanabe N and Price S D 2002 *Meas. Sci. Tech.* **106** 8998
[30] Takahashi J and Uehara H 2001 *Astrophys. J.* **561** 843
[31] Tine S, Williams D A, Clary D C, Farebrother A J, Fisher A J and Meijer A J H M 2003 *Astrophys. Space Sci.* **288** 377
[32] Langmuir I 1918 *Am. Chem. Soc.* **40** 1361
[33] Vidali G, Ihm G, Kim Y S and Cole M W 1991 *Surf. Sci. Rep.* **12** 133
[34] Ghio E, Mattera L, Salvo C, Tommasini F and Valbusa U 1980 *J. Chem. Phys.* **73** 556
[35] Zecho T, Guttler A, Sha X, Lemoine D, Jackson B and Kuppers J 2002 *Chem. Phys. Lett.* **366** 188
[36] Jeloaica L and Sidis V 1999 *Chem. Phys. Lett.* **300** 157
[37] Sha X and Jackson B 2002 *Surf. Sci.* **496** 318
[38] Harris J and Kasemo B 1981 *Surf. Sci.* **105** L281
[39] Jackson B and Lemoine D 2001 *J. Chem. Phys.* **114** 474
[40] Menzel D 1982 in *Chemistry and Physics of Solid Surfaces*, Edited by Vanselow R and Howe R. (Springer Verlag, NY) p. 389
[41] Jennisken P, Blake D F, Wilson M A and Pohorille A 1995 *Astrophys. J.* **455** 389
[42] Jennisken P and Blake D F 1994 *Science* **265** 753
[43] Petrenko V F and Whitworth W 1999 *Physics of Ice* (Oxford University Press)
[44] Vidali G, Roser J E, Manicó G and Pirronello V 2004 *J. Geophys. Res.* **109** E07S14

[45] Perets H B, Biham O, Manicó G, Pirronello V, Roser J, Swords S and Vidali G 2005, submitted for publication.
[46] Verheij L and Zeppenfeld P 1987 *Rev. Sci. Inst. 58* 2138
[47] Hornekaer L, Baurichter A, Petrunin V V, Luntz A C, Kay B D and Al-Halabi A 2005, Preprint.
[48] Diekhoner L, Mortensen H, Baurichter A and Luntz A C 2001 *J. Chem. Phys.* **115** 3356
[49] Katz N, Furman I, Biham O, Pirronello V and Vidali G 1999 *Astrophys. J.* **522** 305
[50] Hollenbach D J and Tielens A G G M 1997 *Annu. Rev. Astron. Astrophys.* **35** 179
[51] Bennet A J, McCaroll B and Messmer R 1971 *Surf. Sci.* **24**, 191
[52] Dovesi R, Pisani C, Ricca F and Roetti C 1976 *J. Chem. Phys.* **65** 3075
[53] Dovesi R, Pisani C and Roetti C 1981 *Chem. Phys. Lett.* **81** 498
[54] Aronowitz S and Chang S B 1985 *Astrophys. J.* **293** 243
[55] Cazaux S and Tielens A G G M 2002 *Astrophys. J.* **575** L29
[56] Cazaux S and Tielens A G G M 2004 *Astrophys. J.* **604** 222
[57] Sha X and Jackson B 2002 *Surf. Sci.* **496**, 318
[58] Sha X, Jackson B and Lemoine D 2002 *J. Chem. Phys.* **116**, 8124
[59] Zecho T, Güttler A and Küppers J 2004 *Carbon* **42**, 6098
[60] Pirronello V, Manicó G, Roser J E and Vidali G 2004 *The Dense Interstellar Medium in Galaxies*, Edited by Pfalzner S et al. (Springer-Verlag, Berlin) p. 525
[61] Buch V and Zhang Q 1991 *Astrophys. J.* **379** 647
[62] Charnley S B, Tielens A G G M and Rodgers S D 1997 *Astrophys. J.* **482** L203
[63] Caselli P, Hasegawa T I and Herbst E 1998 *Astrophys. J.* **495** 309
[64] Shalabiea O M, Caselli P and Herbst E 1998 *Astrophys. J.* **502** 652
[65] Stantcheva T, Caselli P and Herbst E 2001 *Astron. Astrophys.* **375** 673
[66] Biham O, Furman I, Pirronello V and Vidali G 2001 *Astrophys. J.* **553** 595
[67] Green N J B, Toniazzo T, Pilling M J, Ruffle D P, Bell N and Hartquist T W 2001 *Astron. Astrophys.* **375** 1111